

IAC-21-A6,IP,9,x64861

CONSTRAINED OPTIMAL COLLISION AVOIDANCE MANOEUVRE ALLOCATION UNDER UNCERTAINTY FOR SUBSEQUENT CONJUNCTION EVENTS

Luis Sánchez

Aerospace Centre of Excellence, University of Strathclyde, Glasgow, UK,
luis.sanchez-fdez-mellado@strath.ac.uk

Massimiliano Vasile

Aerospace Centre of Excellence, University of Strathclyde, Glasgow, UK, massimiliano.vasile@strath.ac.uk

Abstract

With the increase of the traffic in orbit, there is the need to re-consider the optimisation of Collision Avoidance Manoeuvres (CAM) to account for the occurrence of multiple subsequent conjunction events. This paper proposes a method to compute the optimal CAM for a multiple encounter scenario accounting for operational constraints. The proposed method builds on previous works from the authors where a single CAM was optimised to achieve the required reduction in the Probability of Collision (PoC) under epistemic uncertainty in miss distance and covariance matrices, at the time of closest approach. The uncertainty in the probability of collision derived from the epistemic uncertainty in miss distance and covariance was quantified with Dempster-Shafer theory of evidence (DSt). Within the framework of DSt we defined families of uncertain ellipsoids, with associated probability assignments, that represent all possible relative positions of two objects. CAMs are then optimised to minimise the Probability of Collision for the uncertain ellipse that would yield the highest PoC.

This paper extends this technique by computing the optimal strategy when more than one event with the same object is possible within a given time window. We consider both single and multi-CAM strategies. In both cases, there is a trade-off between the risk of the subsequent encounters, the complexity of the strategy (one or more manoeuvres), the cost and the inherent risk of the manoeuvre. Thus, the computation of an optimal CAM under several encounters requires the solution of a min-max optimisation problem.

In addition, actual missions may present constraints on the execution of the CAM. First, we show how to derive the families of ellipsoids with their associated probability assignment. We then formulate the above-mentioned min-max optimisation to incorporate operational constraints on the multi-encounter scenario. In particular, we consider constraints on execution time or on the magnitude and direction of the manoeuvre. Finally, we incorporate the new multi-CAM optimisation in the framework of CASSANDRA (Computer Agent for Space Situational Awareness aNd Debris Remediation Actions) to automatically allocate CAM and provide operational support to operators by using Multi-Criteria Decision-Making (MCDM) methods. Some representative examples illustrate the applicability of our approach.

keywords: Multiple encounters, Decision-making, Epistemic uncertainty, Collision Avoidance Manoeuvre, Space Traffic Management, Multi-Criteria Decision-Making

CAM Collision Avoidance Manoeuvre
bpa basic probability assignment
DSt Dempster-Shafer theory of evidence
ICS Intelligent Classification System
LT Low-Thrust
MC Manoeuvre cost
MCDM Multi-Criteria Decision-Making
ML Machine Learning
MR Manoeuvre risk
OpC Operational cost
PcR Probability of Collision Reduction

PoC Probability of Collision
SEM Space Environment Management
STM Space Traffic Management
TOPSIS Technique for the Order of Preference by Similarity to the Ideal Solution
WPM Weighted Product Method
WSM Weighted Sum Method

1. INTRODUCTION

While the space traffic is experiencing a dramatic growth during the last years,¹ the Space Traffic Management (STM) system is under an increasing pres-

sure to ensure the space environment safety. The high number of operational satellites and pieces of space debris translates in a raise on the close events alerts. A particular kind of conjunction an operational satellite may trigger is that one involving subsequent encounters, either with the same object or with several ones. These multiple encounter events are likely to occur more often in the future and their adequate treatment is critical for the sustainability of the Earth's orbiting environment.

In addition to this, the STM system has to ensure and adequate treatment of the uncertainty affecting the objects' position. Usually, uncertainty has been assumed to be purely aleatory, but this has been proved to be inadequate.² The epistemic uncertainty, that one related with the lack of knowledge of the system and not with its randomness, should be considered along with aleatory uncertainty. Continuing authors' previous lines of investigation,³ we use Dempster-Shafer theory of evidence (DSt)⁴ to model uncertainty. According to this theory, the uncertain variables defining the position are provided as intervals, thus, the traditional uncertain ellipsoid translates into a family of ellipsoids.

This implies the Collision Avoidance Manoeuvre (CAM) optimisation processes has to be robust, meaning they have to optimise the Probability of Collision (PoC) of the worst-case scenario, which is the ellipsoids within the family of ellipsoids possessing the highest risk. In this paper, we propose to extend the method presented in Sanchez and Vasile⁵ to compute robust optimal CAM to address multi-encounter events affected by aleatory and epistemic uncertainty.

Along with this method, a decision-making support tool for helping on the decision to execute CAMs, firstly presented in previous authors' works,^{3,6} is further developed to cope with new constraints, including those generated for a multiple encounter, and to allocate manoeuvres. A new level of decision making is activated when a manoeuvre should be implemented and provides a list with the best options to allocate CAMs. This system is based on Multi-Criteria Decision-Making (MCDM)⁷ techniques that rank the best optimal alternatives found to avoid the multiple encounter. Thus, a two-level decision-making system is proposed to support operators on the event of a close encounter: first, a Machine Learning (ML)-based classification system to decide whether a manoeuvre or more observations are required to address close encounters, and second, if a CAM is needed, a MCDM-based system to provide

to the operator with the best manoeuvre strategies. This system is integrated in CASSANDRA (Computational Agent for Space Situational Awareness and Debris Remediation Automation), an intelligent agent developed by the Aerospace Centre of Excellence at the University of Strathclyde to handle Space Environment Management (SEM) problems.

The rest of the paper is structure as follows: in Section 2, the robust CAM optimisation method used on this paper is presented. The multiple encounter analysis is included in Section 3. Section 4 extend the intelligent decision-making system to allocate CAM accounting for constraints and multiple encounters and Section 5 includes some numerical examples that illustrates the operation of the system. The final remarks appear in Section 6.

2. ROBUST CAM OPTIMISATION

In this section, the robust CAM optimisation method to deal with close encounters affected by epistemic uncertainty, introduced in Sanchez and Vasile,⁵ is presented.

2.1 CAM linear model

The linear model used on this paper, in Eq. (1), relates the change of velocity due to the manoeuvre, $\delta\mathbf{v}$, with the change on the objects' relative position at the impact plane (also known as b-plane), $\delta\mathbf{x}_b$.

$$\delta\mathbf{x}_b = [\delta\xi \ \delta\eta \ \delta\zeta] = \mathbf{T}\delta\mathbf{v} = \mathbf{BA}(t_m, t_c)\mathbf{G}\delta\mathbf{v}, \quad [1]$$

where \mathbf{G} relates the change of velocity of the primary object at the manoeuvre with the change on Keplerian elements, $\mathbf{A}(t_m, t_c)$ is the transition matrix between the variation in Keplerian elements at manoeuvre time, t_m , and the variation in position at encounter time, t_c , expressed in the satellite's centred <R,T,H> reference frame, and \mathbf{B} is the rotation matrix between the <R,T,H> and the b-plane reference frame. The matrix \mathbf{T} is the product of the three matrices. The expression for matrices $\mathbf{A}(t_m, t_c)$ and \mathbf{G} can be found in Vasile and Colombo.⁸ The b-plane reference frame is centred at the secondary satellite and defined as:

$$\hat{\boldsymbol{\eta}} = \frac{\mathbf{v}_1 - \mathbf{v}_2}{\|\mathbf{v}_1 - \mathbf{v}_2\|}, \quad \hat{\boldsymbol{\xi}} = \frac{\mathbf{v}_2 \times \boldsymbol{\eta}}{\|\mathbf{v}_2 \times \boldsymbol{\eta}\|}, \quad \hat{\boldsymbol{\zeta}} = \hat{\boldsymbol{\xi}} \times \hat{\boldsymbol{\eta}} \quad [2]$$

2.2 CAM optimisation

The optimal CAM is the one providing the minimum PoC at the encounter for the worst-case scenario. In this paper, we assumed the short-term encounter hypothesis hold:⁹ i) rectilinear relative trajectories, ii) no uncertainty in the velocity vector, iii)

the uncertainty in the position of the two objects is Gaussian and uncorrelated, iv) and the shape of the two objects is spherical. Thus, the PoC will reduce to a 2D integral:

$$P_C = \frac{1}{2\pi\sqrt{\|\bar{\Sigma}\|}} \int_{B((0,0),R)} e^{-\frac{1}{2}((\mathbf{b}-\bar{\mathbf{r}}_e)^T \bar{\Sigma}^{-1}(\mathbf{b}-\bar{\mathbf{r}}_e))} d\xi d\zeta, \quad [3]$$

where $\mathbf{b} = [\xi, \zeta]^T$, the two-components vector $\bar{\mathbf{r}}_e$ is equal to the first and third components of \mathbf{r}_e , the miss distance vector expressed on the b-plane reference frame, and $\bar{\Sigma}$ is a 2×2 matrix equal to the first and third elements of the first and third rows of Σ :

$$\bar{\Sigma} = \begin{bmatrix} \sigma_\xi^2 & \sigma_{\xi\zeta} \\ \sigma_{\xi\zeta} & \sigma_\zeta^2 \end{bmatrix},$$

being $\Sigma = \Sigma_{1_{B_p}} + \Sigma_{2_{B_p}}$ the combined covariance matrix of the two objects projected onto the impact plane.

The optimal CAM accounts for both aleatory and epistemic uncertainty. We use DSt⁴ to model it. According to this theory, the uncertain variables are interval-valued. The uncertain variables we consider in this paper are the components of the miss distance and the terms of the covariance matrix: $\mathbf{u} = [\mu_\xi \ \mu_\zeta \ \sigma_\xi^2 \ \sigma_\zeta^2 \ \sigma_{\xi\zeta}]^T$. The fact that the uncertain vector's components are interval valued implies that there is no a single well-defined uncertain ellipse on the b-plane, but a family of them.³ The robust optimisation find the optimal impulse for the ellipse with higher PoC (the worst-case scenario) among those in the family of ellipses ($\Omega_{\mathbf{u}}$) by solving the following min-max problem:

$$\begin{aligned} & \min_{\delta\mathbf{v}} \max_{\mathbf{u} \in \Omega_{\mathbf{u}}} P_C \\ & s.t. \\ & \mathbf{r}_e \cdot \delta\mathbf{v} > 0 \end{aligned} \quad [4]$$

An iterative method included in Sanchez and Vasile⁵ is required to solve it. It is possible to optimise also the impulse magnitude. We assumed the manoeuvre does not introduce further uncertainty and only translates rigidly the uncertain ellipses in the impact plane. In his work, we have restricted the analysis to the impulsive scenario, but the method can handle also the Low-Thrust (LT) case.

3. MULTIPLE ENCOUNTERS

A multiple encounter is a series of successive close conjunctions between one satellite and one or more space objects, whether operational satellites or pieces of space debris.

The individual encounters in a multiple event can be catalogued as follows:

- Primary encounter, the first conjunction between Object A (i.e. operational satellite) and Object B (i.e. another satellite or a piece of space debris).
- Secondary encounter, a second conjunction between Object A and Object B.
- Tertiary encounter, an encounter between Object A and Object C (i.e. another satellite or piece of space debris) taking place after the primary encounter.

3.1 *Avoiding strategies*

Next, we propose different approaches to address the multi-encounter events.

3.1.1 *Single manoeuvre strategies*

On the first place, the multiple encounters can be tackled with a single manoeuvre. This approach presents some advantages, as the fact that a single manoeuvre presents less operational limitations, but can restrict the optimality of the solution.

The simplest approach is to optimise the impulse according exclusively to the primary encounter. Since it is the first encounter on time to be faced by the operational satellite, this approach prioritised the urgency of the event. Another possibility is to optimise the event possessing the highest risk, whether is the first or any subsequent encounter. In any case, only one manoeuvre is performed and the optimisation is straightforward, since only information from one encounter should be considered.

Thus, the optimal impulse is obtained by solving Eq. (4), where $\Omega_{\mathbf{u}}$ is composed only for the family of ellipses of the conjunction considered. The main disadvantage of this approach is that, while the risk of one of the events is adequately reduced, the other events are not included at all on the optimisation process and they may not experience a reduction on their risk.

Another approach that only involves one manoeuvre is to optimise all encounters simultaneously. Assuming all the events involve the same pair of objects, their uncertainties are correlated and they can be added together. Thus, the set $\Omega_{\mathbf{u}}$ is now constituted by the set of families of all the encounters, increasing in size accordingly.

The solution of the process is an impulse that optimises the worst-case scenario of the combined event. This method presents the advantages of being robust

and the simplicity of a single manoeuvre (which is important from the operators perspective). However, the impulse may not be optimal from the point of view of each individual encounter: the worst-case scenario of each encounter may present a higher PoC compared to the individual optimisation of each individual conjunction (next strategy).

3.1.2 *Multiple manoeuvres strategies*

A different strategy is to execute a manoeuvre for each of the individual encounters on the multiple event. On the one hand, this presents the advantage that it is each event which is optimised, and not the combination of them, solving the main disadvantage of the previous approach. On the other hand, more than one manoeuvre is required, introducing complication to the operations (more than one slot has to be allocated), there is a higher risk and cost associated to the manoeuvres executions, and new constraints on the execution of the secondary manoeuvres, which have to be executed after the previous encounters, are introduced. Moreover, several optimisation runs has to be carried out, one per manoeuvre. However, if the risk of all the events is further reduced, this strategy may be justified.

To obtain the optimal impulse the process is different for the primary encounter than for the subsequent encounters. The impulse for the first encounter is obtained by solving Eq. (4) as in the first strategy. For the next conjunction, the new relative position after executing the previous manoeuvre has to be obtained, which will modify the encounter geometry and the PoC respect to the unperturbed scenario. The new position will depend on when the previous impulse has been executed. Once computed the new position, the optimal impulse for the secondary encounter is obtained by solving again Eq. (4).

4. CAM ALLOCATION

In this section, a system to support on the allocation of manoeuvres, accounting for epistemic and aleatory uncertainty, multiple encounters and operational constraints is presented.

This system aims to support operators on the decision-making task during conjunction events. It is divided in two level of decision: in the first one, the system provides the most suitable action to be carried out (execute a manoeuvre, obtain more measurement or not take further actions) according to the evidence supporting the risk of the event; the second level of decision intervene when a CAM is recommended by the previous level. It considers constraints on the ma-

noeuve (operational, magnitude, direction...) and proposes a ranked list of possible CAMs and their execution position. Fig. 1 shows the architecture of the system.

4.1 *Intelligent Classification System*

The Intelligent Classification System (ICS) represents the first level of decision-making. This system is a ML-based classifier that proposes the most suitable action to be taken by the operators on the event of a close encounter. It was trained according to the epistemic event classification criterion in Table 1. It takes into account the time to the encounter and the confidence (*Belief* and *Degree of Uncertainty*) on the value of the PoC according to the available information. More details can be found in Sanchez and Vasile.³

Table 1: Epistemic classification criterion. More information in Sanchez and Vasile.³

Time to TCA	PoC for $Bel _{P_C} = Bel_0$	DoU at P_{C0}	Class
$t_{TCA} < T_1$	$P_{Cb} \geq P_{C0}$	-	1
	$P_{Cb} < P_{C0}$	$DoU _{P_{C0}} \leq \Delta$ $DoU _{P_{C0}} > \Delta$	5 1
$T_1 \leq t_{TCA}$ $t_{TCA} < T_2$	$P_{Cb} \geq P_{C0}$	-	2
	$P_{Ce} < P_{C0}$	$DoU _{P_{C0}} \leq \Delta$ $DoU _{P_{C0}} > \Delta$	5 3
$T_2 \leq t_{TCA}$	$P_{Cb} \geq P_{C0}$	-	2
	$P_{Cb} < P_{C0}$	$DoU _{P_{C0}} \leq \Delta$ $DoU _{P_{C0}} > \Delta$	4 3

The ICS takes as inputs the uncertain variables of the encounter geometry (miss distance and covariance matrix), the time to the encounter and the confidence on the source of information. More than source can provide information, i.e. different sensors. It classify the event a one of the five possible classes, which have a required action associated:

- *Class 1*: perform a manoeuvre,
- *Class 2*: design/prepare a manoeuvre, but collect more information if possible before executing it,
- *Class 3*: collect more measurements,
- *Class 4*: low risk event, no need to prepare a manoeuvre, although collecting more information would be beneficial to confirm the decision,

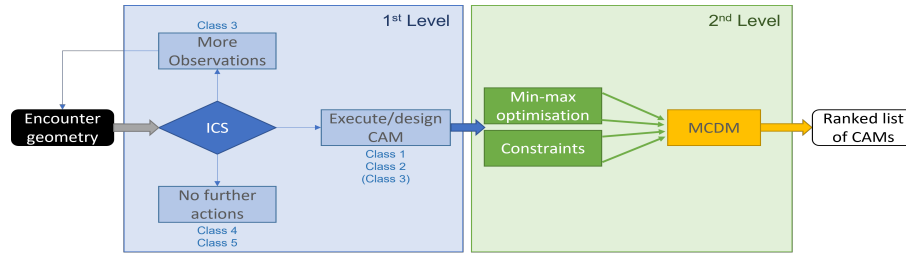


Fig. 1: Pipeline of the decision-making system.

- *Class 5*: not perform any action.

If the event is categorised as *Class 1* or *Class 2*, the next level of decision starts. Although a *Class 3* event does not necessarily require a CAM, they will also activate the next level. In case of a multiple encounter, the second level starts if at least one of the conjunctions is classified as *Class 1*, *Class 2* or *Class 3*.

4.2 Constraints

After the first level of decision-making, when a CAM is required, a list of possible solutions should be proposed. These solutions are robust optimal manoeuvres that vary by the execution position or by the strategy followed in the case of a multiple event (one or more manoeuvres), but some constraints may affect the solutions. Thus, before activating the second level of decision-making, an intermediate step should be included to account for the relevant constraints.

On this work, we address three types of constraints on the manoeuvres: constraints related to the magnitude, to the direction and to the execution time/position. In the following, a more detailed explanation of these constraints is presented.

Magnitude constraints These constraints are related to whether the magnitude can be modified or not

- *Magnitude variation.* This constraint refers to the fact that certain missions present more limited manoeuvre capabilities and cannot change the magnitude of the thruster. If this constraint applies, Eq. (4) has to be solved indicating the value of the impulse $\delta\mathbf{v} = \delta\mathbf{v}_0$.
- *Magnitude optimisation.* On the other hand, if the satellite can vary the magnitude of the manoeuvre, it could be possible to optimise this value to save fuel so that $P_C \leq P_{C0}$, being P_{C0} the PoC safety threshold aiming to reach with the CAM. The algorithm to address this scenario is presented in Sanchez and Vasile.⁵

Direction constraints Depending on the type of satellite and the objective of its mission, the manoeuvres directions can be restricted to certain configurations, i.e. limited attitude control capabilities, minimising impact on the mission objectives, avoiding certain instruments alignments (star-trackers and sun)...

- *Restricted direction.* In order to make the manoeuvre simple or due to operational/mission considerations, the manoeuvre is required to be executed in a specific direction (i.e. tangential impulse) instead of the optimal one. This situation simplifies the optimisation algorithm: the iterative process presented in Sanchez and Vasile⁵ is no longer required. Instead, only the worst-case scenario after applying the restricted manoeuvre should be computed (the maximisation step on the min-max problem):

$$\max_{\mathbf{u} \in \Omega_{\mathbf{u}}} (P_C | \delta\mathbf{v})$$

- *Range of available/forbidden directions.* In other situations, the pointing constraints are less hard or there are only limited angles that are restricted. In this situation, the min-max problem in Eq. (4) need to be solved, but additional requirement should be included during the minimisation step to exclude from the solution the angles out of the validity range.

Execution time/position It is a common practise among operators to restrict the time or position execution of the manoeuvres, specially, allowing time between to ensure communication windows before the encounter.¹⁰ In other circumstances, they would restrict the manoeuvre execution to instants where the satellite is visible. It is also usual to avoid certain orbital regions: eclipses, South-Atlantic anomaly... Finally, in multi-encounter events, the events themselves may include constraints.

- *Relative position.* This constraint refers to the relative position between the manoeuvre execution and the encounter. As mentioned, some operators want to keep certain time or number of orbits between the execution of the manoeuvre and the encounter in order to make the necessary status checks to confirm the correct execution of the CAM. This constraints means that the optimisation problem is solved only for values of $\Delta\theta_m > \Delta\theta_{m0}$, being $\Delta\theta_{m0}$ the latest position with respect to the encounter to perform the impulse.
- *Absolute position.* Contrary to the previous constraint, this one refers to the position of the manoeuvrable satellite with respect to the Earth, Sun or other objects. Some operators prefer to avoid certain regions when executing the manoeuvre: eclipses, South-Atlantic anomaly, communication passes... Similarly to the previous constraints, this implies that the solution of the optimisation problem is not computed or the solution is excluded if the satellites is located in this restricted areas.
- *Time.* This constraints is similar to the previous one, but referring to the time a which the manoeuvre is executed. Certain times may want to be avoided, for example, non-working hours at the operations centre to reduce operational costs. This constraints translates, as above, in excluding those positions associated with the restricted times from the optimisation.
- *Multiple encounters.* This constraints is associated to the relative distance between encounters. If only one manoeuvre is required, this constraints does not apply. However, if each encounter is avoided with a dedicated CAM, the first encounters may affect the execution time/positions of subsequent manoeuvres. The most obvious constraints is not to perform a manoeuvre after the previous encounter has been avoided. Thus, only optimal positions computed between encounters would be candidates for the second (or subsequent) encounter if a multi-manoevrue strategy is chosen.

4.3 *Multi-Criteria Decision-Making System*

Once those events requiring a CAM are identified during with the ICS and the different optimal alternatives (CAMs with different execution times and different multi-encounter strategies) have been computed

accounting for the relevant constraints, the second level of decision-making is activated.

The objective of this second level is to support operators providing a list with the best avoiding strategies with respect to some risk and cost criteria. Those alternatives are ranked, so not only the most optimal solution is presented, but also other options so the operator can make the final decision. This system uses MCDM methods.

MCDM is a branch of decision making which involved procedures to deal with decision problems, so it provides a compromise solution (in the form of a sorted list) of alternatives evaluated across a set of, usually contradictory, criteria.¹¹ Hence, there are three type of parameters that should be defined in order to apply the different MCDM methods: the alternatives, the criteria and the weight of the criteria.

Alternatives The alternatives are the different solutions obtained through solving the optimisation problem. In this work, each alternative is defined by the execution position, $\Delta\theta_m = \theta_c - \theta_m$, measured as the difference between the manoeuvre execution position and the encounter, and the CAM (direction and impulse), $\delta\mathbf{v}$, defined in the satellite's <T,N,H> reference frame for each of the manoeuvres the selected strategy requires: $\mathcal{A} = (\Delta\theta_{m,i}, \delta\mathbf{v}_i | i = 1, \dots, N_{man})$.

Thus, for a multi-encounter event, the set of alternatives comes from obtaining the robust optimal CAM at different positions using the strategies in Section 3.1.

Criteria The criteria are the indicators use to assess the preference of one alternative above the others. In general, the criteria present conflict among them and some alternatives perform better on some criteria while other solutions score better on others. The criteria can be classified as *Beneficial* criteria, those to be maximised, and *Non-Beneficial* or *Cost* criteria, which have to be minimised. In this work, we have considered four criteria, two cost-wise and two risk-wise, Fig. 2.

- *Probability of Collision Reduction (PcR).* It is a measurement related with the risk of the encounter. It indicates how much the proposed alternative reduced the PoC respect the no-manoevrue case, $P_{C, nm}$. It is a *Beneficial* criterion modelled with a monotonic decreasing function ranging in the interval [0,1]. Those manoeuvres that do not improve or worsen the initial PoC are scored as 0. In the contrary, the manoeuvres that reduced the PoC below the safety threshold P_{C0} are scored as 1. Several func-

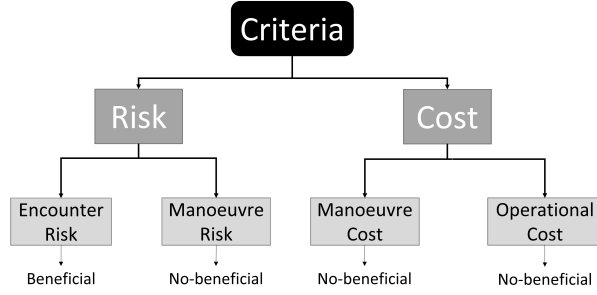


Fig. 2: MCDM criteria, their classification and their quantification.

tions can accomplish these conditions, as shown in Fig. 3. Since we want to prioritised manoeuvres that reduce the probability of collision close to or below the threshold, we selected the *Alternative 4* in Fig. 3:

$$PcR = \left(\frac{\log_{10} P_C - \log_{10} P_{C,nm}}{\log_{10} P_{C0} - \log_{10} P_{C,nm}} \right)^{16}.$$

- *Manoeuvre risk (MR)*. Since the manoeuvre execution poses an inherent risk, this criterion prioritised those strategies that involved less manoeuvres. It is a *Non-Beneficial* criterion modelled as:

$$MR = N_{man}/N_{enc},$$

where N_{man} is the number of manoeuvres required and N_{enc} the number of encounters on the event. While more manoeuvres than encounter are possible, in this work, we limited the manoeuvres to a maximum of one per encounter ($MR \in [0, 1]$).

- *Manoeuvre cost (MC)*. The cost of the manoeuvre refers to the amount of fuel required, which is directly related with the magnitude of the impulse. Thus, we modelled this *Non-Beneficial* criterion as the sum of the impulses of the strategy, normalised with the maximum capacity of the thrust at each manoeuvre:

$$MC = \sum_{n=0}^{N_{man}} \frac{\delta v_n}{\delta v_{n,max}}.$$

- *Operational cost (OpC)*. This criterion refers to the cost associated to placing the satellite out of the nominal orbit. Ideally, from the mission goals perspective, the manoeuvre should be implemented as close as possible to the encounter, since the disruption of the mission

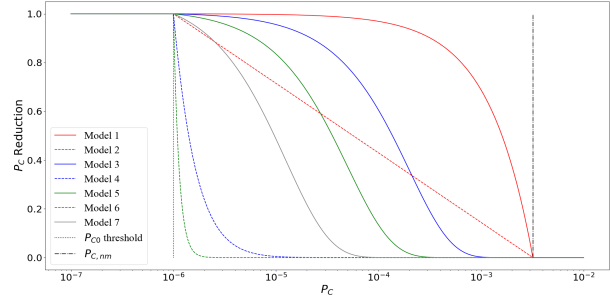


Fig. 3: Set of possible linear and potential functions to model the PcR. Solid lines: in linear scale. Dashed lines: in logarithmic scale. Selected model: *Model 4* (blue dashed line). Black vertical lines: $P_{C,nm}$ in pointed-dashed and P_{C0} in pointed.

will be smaller. Thus, we modelled this *Non-Beneficial* criterion as the arc-length the satellite is away from the nominal position due to the manoeuvre, normalised with the maximum arc-length among all the alternatives:

$$OpC = \frac{\Delta\theta_{m,1}}{\max_i(\Delta\theta_{m,1})}, \quad i = 1, \dots, N_{alt},$$

with N_{alt} the number of alternatives. Some considerations on this criterion. In this work, only the period away of the nominal orbit before the encounter is considered and we assume the satellite does not return to the nominal orbit until the last encounter has been avoided. Thus, only the arc-length before the primary encounter, $\Delta\theta_{m,1}$, may differentiate one alternative from the others.

Weights and normalisation The weights allow to define the relative importance of the criteria when the alternatives are evaluated with the models. In general, they are normalised so that $\sum_j^{N_{crit}} w_j = 1$, being N_{crit} the number of criteria. The weight distribution along the criteria has an effect on the final ranking. The alternatives, criteria and weights allow to obtain the weighted Decision matrix that includes the value of the alternative i^{th} with respect to the criterion j^{th} balanced with the associated weight.

Another aspect that may influence the final rank is the normalisation of the alternatives. In general, the criteria can have different units or different range of values. Most of the methods require that they have comparable values in order to provide meaningful results. Thus, a normalisation process has to be carried out on the Decision matrix, but different normalisation techniques outcomes different normalised

matrices. In this work, we used the following normalisation linear model:¹²

$$\begin{cases} \text{if } \textit{Beneficial} \text{ crit.:} & \bar{a}_{ij} = a_{ij} / \max_i(a_{ij}) \\ \text{if } \textit{Non-Beneficial} \text{ crit.:} & \bar{a}_{ij} = \min_i(a_{ij}) / a_{ij} \end{cases}, \quad [5]$$

with $i = 1, \dots, N_{alt}$ and where a_{ij} and \bar{a}_{ij} are the value of the i^{th} alternative with respect to the j^{th} criterion on the Decision matrix, non-normalised and normalised, respectively. This method avoids to normalised to 0 the worst alternative in each criteria (which is positive, and even required, in some methods) and transforms all the criteria into *Beneficial* criteria.

Methods Once the Decision matrix is obtained and the criteria weights defined, it is possible to rank the solutions by applying one of the several methods available on the literature.¹³ In this work, we have limited our analysis to: Weighted Sum Method (WSM),¹⁴ Weighted Product Method (WPM),¹⁵ Technique for the Order of Preference by Similarity to the Ideal Solution (TOPSIS).¹⁶ On the following, we provide a brief explanation of each to them.. Note: in the following equations, for all the methods: $i, k = 1, \dots, N_{alt}$ and $j = 1, \dots, N_{crit}$, where N_{alt} is the number of alternatives, N_{crit} the number of criteria.

- *WSM* On of the simplest MCDM methods. It is based on the utility add hypothesis. The weighted values of the alternatives with respect to the criteria are added. The alternative with the highest added value ranks first. If the variable presents different units' range, normalisation schemes are required.

$$A_{i,WSM} = \sum_{j=1}^{N_{crit}} w_j * a_{ij}.$$

- *WPM* This method is similar to WSM, but instead of adding the values, it compares each solution to the all the others using a multiplication of weighted ratios:

$$P_{ik,WPM} = \prod_{j=1}^{N_{crit}} \left(\frac{a_{ij}}{a_{kj}} \right)^{w_j},$$

where $P_{ik,WPM} > 1$ indicates the i^{th} alternative is better than the k^{th} alternative. The above equation does not rank the alternatives but just provide a new matrix, \mathcal{P} , with size $[N_{alt} \times N_{alt}]$. To sort the solutions, the alternative with a

higher number of elements on its row greater than one ranks first:

$$A_{i,WPM} = \text{count}_k(P_{ik,WPM} \geq 1).$$

If normalisation techniques are applied to the Decision matrix, care should be taken to avoid zeros on the matrix.

- *TOPSIS* As its name suggests, this method is based on finding the best solution according to the distance to some ideal best and worst alternatives. From the normalised and weighted Decision matrix, the ideal best and ideal worst solution can be obtained as:

$$A^+ = \left\{ \max_j(a_{ij}) \text{ if } j \in C^+, \min_j(a_{ij}) \text{ if } j \in C^- \right\},$$

$$A^- = \left\{ \min_j(a_{ij}) \text{ if } j \in C^+, \max_j(a_{ij}) \text{ if } j \in C^- \right\},$$

whit C^+ the set of *Beneficial* criteria and C^- the set of *Non-Beneficial* criteria. Then, the method ranks the solutions based on the geometrical distance between each alternative and the ideal alternatives:

$$A_{i,TOPSIS} = \frac{D_i^-}{D_i^+ + D_i^-},$$

where

$$D_i^* = \sqrt{\sum_{j=1}^{N_{crit}} (a_{ij} - a_j^*)^2}, \text{ and } * = \{+, -\},$$

being a_j^+ and a_j^- the elements of A^+ and A^- , respectively. The solution with higher $A_{i,TOPSIS}$ ranks first.

5. NUMERICAL CASE

In this section, we introduce two numerical examples to show the operation of the decision-making support system under the event of a multiple encounter. Given the initial state of two objects and their associated uncertainty (aleatory and epistemic), the multiple encounters are detected and the confident on their risk computed. The decision-making system is then activated: initially, the ICS evaluates each event and determines the necessity or not of implementing a CAM. If any of the encounters requires an orbit correction, the second level of the decision-making system is activated. Different optimal robust manoeuvres are computed following the different strategies presented for multiple encounters

in Section 3, accounting for the corresponding constraints, and MCDM methods are employed to rank the alternatives in order to provide the best ones to the operators.

In these examples, we only consider encounters between two space objects, where Object A represents a manoeuvrable operational satellite assumed to be perfectly known, and Object B a piece of space debris whose position is known with uncertainty; and only the primary encounter a one secondary encounter are analysed.

In the first examples, both encounters take place in the same orbit region, while in the second case, the second encounter occur in the opposite site of the orbit. This will have an impact on the suitability of the alternatives and it will test the decision support system under two very different situations.

Keplerian motion is assumed in both examples, the short-encounter hypothesis holds and the CAM is considered to just translate rigidly the uncertain ellipses, no changing their shape, size or orientation.

5.1 *Example 1*

5.1.1 *Initial state and encounter detection*

We assume two space objects following a multiple-encounter trajectory. The primary object represents an operational satellite with manoeuvre capabilities whose position is perfectly known. The other object, the secondary, is a piece of space debris whose position is known with uncertainty. The initial states of both objects at a time t_0 are included on Table 2. Note: the piece of space debris has a period 5 times greater than the operational satellite.

Table 2: Nominal Keplerian elements at initial time.

Variable	Unts.	Obj. 1	Obj. 2 (Ex. 1)	Obj. 2 (Ex. 2)
SMA (a)	[km]	7,100.0	20,760.53	7,100.05
Ecc. (ecc)	-	10^{-5}	0.658	10^{-5}
Incl. (i)	[rad]	$\pi/4$	$2/3\pi$	$\pi/3$
RAAN (Ω)	[rad]	0.0	0.0	π
Arg. p. (ω)	[rad]	0.0	0.0	π
TA (θ)	[rad]	$\pi/2$	3.9723	$\pi/2$

The uncertainty on the secondary's initial position has two components: aleatory and epistemic. The aleatory term is modelled with a 3D Gaussian distribution, expressed on the object's <T,N,H> reference frame: $\mathcal{N}_3(\boldsymbol{\mu}_{tnh_0}, \boldsymbol{\Sigma}_{tnh_0})$. The epistemic uncertainty is modelled using DSt. Thus, the epistemic compo-

nent provides a set of two interval-valued epistemic parameters: $\boldsymbol{\lambda} = [\boldsymbol{\lambda}_\mu, \boldsymbol{\lambda}_\sigma] = [[\underline{\boldsymbol{\lambda}}_\mu, \overline{\boldsymbol{\lambda}}_\mu], [\underline{\boldsymbol{\lambda}}_\sigma, \overline{\boldsymbol{\lambda}}_\sigma]]$, such that:

$$\boldsymbol{\mu}_{tnh} = \boldsymbol{\mu}_{tnh_0} + \boldsymbol{\lambda}_\mu,$$

$$\boldsymbol{\Sigma}_{tnh} = \begin{bmatrix} \sigma_{t_0}^2 \lambda_{\sigma_t} & 0 & 0 \\ 0 & \sigma_{n_0}^2 \lambda_{\sigma_n} & 0 \\ 0 & 0 & \sigma_{h_0}^2 \lambda_{\sigma_h} \end{bmatrix}.$$

The uncertain initial position of the secondary object can be defined as $\mathbf{x}_{tnh_0} = \mathcal{N}_3(\boldsymbol{\mu}_{tnh_0}, \boldsymbol{\Sigma}_{tnh_0}; \boldsymbol{\lambda})$. Since DSt allows to include more than one source of information, we assumed two equally-reliable sources providing conflict information are available. Thus, two set of epistemic parameters are provided. The values of the initial uncertainty are shown in Table 3. More information on how to model the uncertainty can be found in Sanchez and Vasile.⁵

Table 3: Secondary object's initial uncertainty.

Aleatory uncertainty: nominal position, $\boldsymbol{\mu}_{tnh_0}$, and diagonal covariance matrix, $\boldsymbol{\Sigma}_{tnh_0}$, on its <T,N,H> reference frame. Epistemic uncertainty: two sources of information providing the interval-valued parameters, $\boldsymbol{\lambda}_\mu, \boldsymbol{\lambda}_\sigma$, that modify the mean and the covariance matrix elements. Note: $\lambda_{\mu_t} = \lambda_{\mu_n} = \lambda_{\mu_h}$ and $\lambda_{\sigma_t} = \lambda_{\sigma_n} = \lambda_{\sigma_h}$.

Aleatory	Units	Example 1	Example 2
$\boldsymbol{\mu}_{tnh_0}$	[km]	[0, 0, 0]	[0, 0, 0]
$\sigma_{t_0}^2$	[km ²]	0.1 ²	0.05 ²
$\sigma_{n_0}^2$	[km ²]	0.1 ²	0.05 ²
$\sigma_{h_0}^2$	[km ²]	0.1 ²	0.05 ²
Epistemic (Examples 1 & 2)		Source 1	Source 2
λ_{μ_i}	[km]	[0.00, 0.01]	[-0.53, -0.515]
λ_{σ_i}		[1,4]	[1/5, 1/2]

The nominal position is propagated in interval of time T_{inter} where some close encounters are detected. A close encounter is defined when the nominal relative distance between both objects is smaller than a selected threshold: $D \leq D_0 = 10km$. As indicated before, only primary and secondary encounters are considered. The primary encounter is located at $t_1 = 34,235$ s from the initial time (5.75 revolutions for the primary satellite after the initial time) and the secondary encounter at $t_2 = 64,004$ s (5 revolutions after the primary encounter for the operational satellite, $\Delta\theta_{1,2} = 10\pi$ rad), with a nominal miss distance of $D_1 = 2.69$ km and $D_2 = 1.33$ km, respectively.

Both encounter take place at the perigee of the orbits.

The initial uncertainty is also propagated to the encounters using a Monte Carlo simulation. From each set of distributions defined by each of the two sources of information, a number of ellipsoids are drawn within the interval limits. Those ellipsoids are sampled and each sample is propagated to the encounter times and projected on the respective impact planes. In this work we assumed the normality of the distributions remains after the propagation, so from each initial ellipsoid, we obtain an uncertain ellipse in the impact plane. Since the primary object is assumed to be perfectly known, the combined covariance matrix at the encounter is equal to the secondary object covariance matrix. At each encounter's impact plane, two sets of uncertain ellipses, associated to each source of information, is obtained. These sets are modelled, according to DSt, with intervals defined by the minimum and maximum values of each of the uncertain variables within the set: miss distance and covariance matrix elements, whose limits are indicated in Table 4.

5.1.2 *Risk assessment and decision-making*

Once the uncertain relative geometry at each of the encounters is obtained, the decision-making system can be activated. Initially, a risk assessment of the multi-encounter event should be performed using the ICS. The ICS used in this work has been previously trained on a synthetic database. The training process is detailed in Sanchez and Vasile.⁵

The ICS takes as inputs the sets of intervals of the uncertain variables defining the geometry of the encounter (Table 4), the time to the encounter (t_1 or t_2), and the reliability of the source, quantified as basic probability assignments (*bpa*).¹⁷ Since both sources of information are assumed to be equally reliable: $bpa_1 = bpa_2 = bpa = 0.5$. It will provide the suggested action to be taken by the operator in relation to each encounter as one of the five classes defined in Section 4.1.

Both encounters are classified as *Class 1*, which means an avoidance manoeuvre should be designed and executed. As mentioned before, if at least one of the encounters is classified as *Class 1, 2* or *3*, as it is the case, the next level of the decision-making system starts.

5.1.3 *CAM allocation and solution ranking*

The first step of the second level of decision-making is to obtain the different alternatives from the solution of the min-max optimisation problem in

Eq. (4) at different execution positions and with the different strategies introduced in Section 3.1.

Before obtaining these solution, some operational constrains are defined:

- Magnitude constraints. The satellite is assumed to provide only a fix-magnitude impulse with value: $\delta v = 16$ cm/s.
- Direction constraints. No direction constraints have been considered on this example.
- Execution time/position constraints. Two constraints of this kind are considered: i) the manoeuvre has to be executed at least 2 orbits before the encounter (this constraints simulates the time left by operator to check the correct implementation of the manoeuvre); ii) and the second execution (when required) has to be implemented after the first encounter ($\Delta\theta_{m,2} < \Delta\theta_{1,2}$).

The alternatives were computed using the three strategies mentioned above: i) computing the CAM that optimises only the first encounter, ii) obtaining the single manoeuvre that optimises simultaneously both encounters and, iii) two manoeuvres, one per each encounter. The manoeuvres are computed at execution positions half a revolution before each encounter for the 10 previous orbits ($\Delta_m = \theta_c - p * \pi$, $p = 1, 3, \dots, 19$), taking into account the restrictions indicated before. Each solution, \mathcal{A} is defined by: the execution positions measured as the angular distance in true anomaly with respect the encounter they are avoiding (if only one manoeuvre, it refers to the primary encounter), $\Delta\theta_m = \theta_c - \theta_m$, the direction of the manoeuvre, $\delta\hat{v}$, expressed in the satellite's <T,N,H> reference frame, and the magnitude of the impulse, for each of the required manoeuvres: $\mathcal{A} = [\Delta\theta_{m,n}, \delta\hat{v}_n, \delta v_n] \mid n = 1, \dots, N_{man}$. Figs. 4a and 4b and Figs. 5a and 5b show, respectively, the evolution of the PoC and the optimal robust CAM for the three selected strategies as a function of $\Delta\theta_{m,1}$ or $\Delta\theta_{m,2}$.

A total of 35 alternatives are obtained, $N_{alt} = 35$. Seven from the first strategy (one manoeuvre optimising the first encounter), 7 from the second strategy (one manoeuvre optimising the two encounters), and 21 from the multi-manoevr strategy. Alternatives are numbered so the first 7 alternatives corresponds to the *Strategy 1*, starting from the manoeuvre executed closer to the encounter, the next 7 correspond to the *Strategy 2* similarly also starting from the execution position closer to the encounter, and the other

Table 4: Bounds of the sources' intervals for the uncertain variables on the impact plane of the two encounters and bounds of the intervals of the associated PoC.

Primary encounter		Example 1		Example 2	
	Units	Source 1	Source 2	Source 1	Source 2
μ_ξ	[km]	[-0.02948, 0.03158]	[-0.01485, -0.09976]	[-0.02948, 0.03158]	[-0.2405, -0.1936]
μ_ζ	[km]	[2.4001, -0.3924]	[12.298, 13.497]	[-1.4605, 1.335]	[12.457, 14.163]
σ_ξ^2	[km ²]	[0.01435, 0.04358]	[2.045, 4.893]·10 ⁻³	[0.01311, 0.06118]	[2.1843, 6.008]·10 ⁻³
σ_ζ^2	[km ²]	[9.258, 39.255]	[1.858, 5.009]	[12.045, 53.657]	[2.4137, 6.5185]
$\sigma_{\xi\zeta}$	[km ²]	[-1.024, -0.1559]	[-0.1247, 2.983]	[0.3298, 1.6396]	[0.0592, 0.1761]
P_C	-	[0.523, 1.382]·10 ⁻⁴	[0.0, 10 ⁻¹³]	[0.574, 1.311]·10 ⁻⁴	[0.0, 0.0]
Secondary encounter					
μ_ξ	[km]	[-0.01978, 0.03996]	[-0.09024, -0.06255]	[0.0351, 0.1214]	[-0.7497, -0.7172]
μ_ζ	[km]	[-4.282, -0.307]	[24.537, 26.855]	[-4.355, 0.9630]	[21.840, 25.081]
σ_ξ^2	[km ²]	[0.01301, 0.04937]	[1.470, 3.907]·10 ⁻³	[0.01559, 0.06119]	[0.8778, 2.3635]·10 ⁻³
σ_ζ^2	[km ²]	[34.391, 152.602]	[6.898, 18.498]	[4.360, 19.430]	[8.735, 23.598]
$\sigma_{\xi\zeta}$	[km ²]	[-2.103, -0.279]	[-0.172, -2.103]	[-3.288, -0.6823]	[-0.1567, -0.0251]
P_C	-	[2.523, 9.152]·10 ⁻⁵	[0.0, 10 ⁻¹²]	[2.453, 9.533]·10 ⁻⁵	[0.0, 0.0]

alternatives are numbered according to the proximity of the first manoeuvre to the primary encounter and, when equal, according to the proximity of the second manoeuvre to the secondary encounter.

Since the magnitude of each individual manoeuvre is the same, the total cost of an alternative will be proportional to the number of manoeuvres, as it does the manoeuvre risk. This means the two criteria are correlated and one can be eliminated, in this case, the Manoeuvre Risk, MR. Since there is two encounters, the risk of each of them is included as a different criteria, thus, the total number of criteria is $N_{crit} = 4$. The safety threshold for the PoC is equal to $P_{C0} = 10^{-6}$. With this information is possible to compute the Decision matrix.

The matrix is normalised using the linear model in Eq. (5). This model considers differently the *Beneficial* and the *Non-Beneficial* criteria, such that the best case within the criteria (maximum score in *Beneficial* criteria and minimum score in *Non-Beneficial* criteria) is normalised to 1.

Two different scenarios are studied: i) an encounter risk prioritising scenario, where the collision risk reduction is assigned a higher weight, and ii) a cost prioritising scenario, which gives a higher weight to the manoeuvre and operational costs. Table 5) includes the weight distribution for each scenario.

As mentioned in the previous section, the ranking process has been carried out using three MCDM methods: WSM, WPM and TOPSIS. Table 6 includes the top-10 alternatives obtained with each

Table 5: Weight distribution for the two analysed scenarios.

Scenario	PcR1	PcR2	MR	MC	OpC
Example 1					
Risk prior.	0.45	0.45	-	0.05	0.05
Cost prior.	0.05	0.05	-	0.45	0.45
Example 2					
Risk prior.	0.4	0.4	0.1	0.05	0.05
Cost prior.	0.05	0.05	0.1	0.4	0.4

method for the two scenarios.

5.2 Example 2

In this section we introduce another example. While the previous one presented the two encounters in the same region of both orbits (around their perigee), in this example, the encounters occurs in two opposite regions of the orbits: perigee and apogee.

The initial position at t_0 of both satellites is included in Table 2. Note: due to the similar semimajor axis and eccentricity, there are close encounters every half orbit. For the purpose of this analysis, we only consider two encounters: the primary encounter occurring at 34,235 s from the initial time with a relative distance of 3.73 km, and the secondary encounter taking place at 66,981 s from the initial time

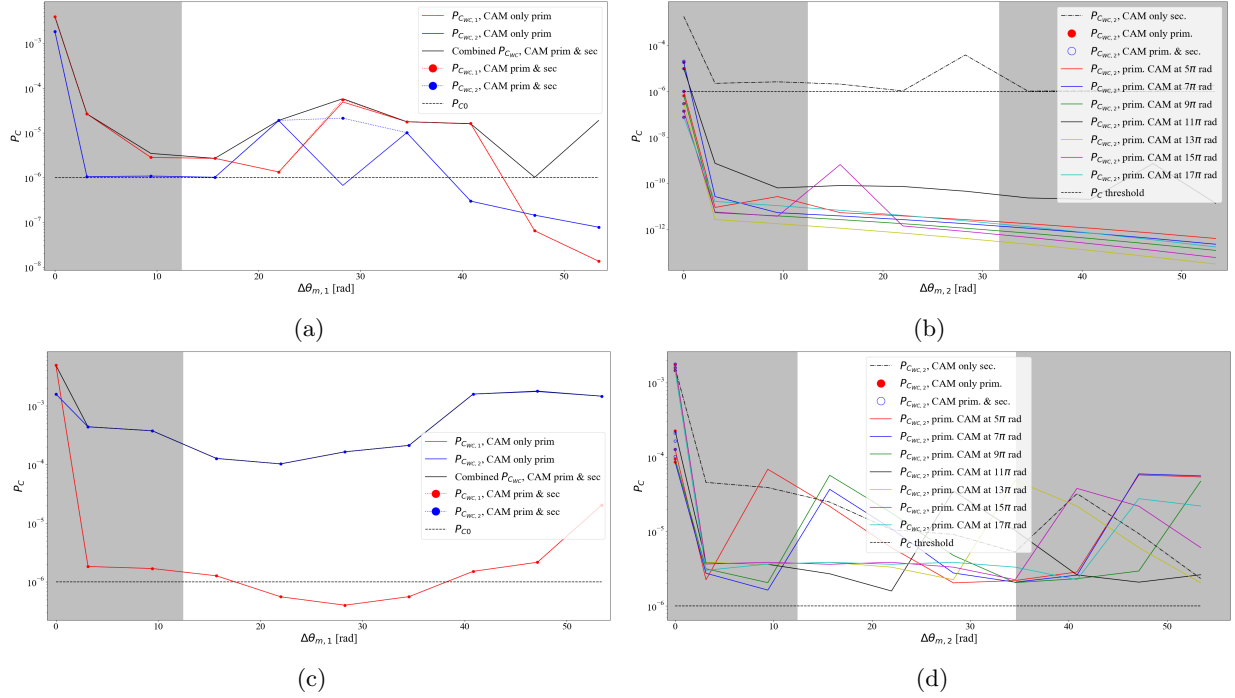


Fig. 4: Evolution of the P_{CWC} for the primary and secondary encounters as a function of the CAM execution positions, $\Delta\theta_m$. (a) and (b) corresponds to the Example 1, (c) and (d) to the Example 2. (a)(c) One manoeuvre strategies: red: primary encounter, $P_{CWC,1}$; blue: secondary encounter, $P_{CWC,2}$; solid lines, only optimising the primary encounter; pointed lines/circles, optimising the primary and secondary encounters simultaneously. Solid black line, P_{CWC} of the primary and secondary combined scenario; dashed black line, PoC safety threshold, P_{C0} ; shaded region, manoeuvres violating the position constraints ($\Delta\theta_{m,1} < 4\pi$). (b)(d) $P_{CWC,2}$ after the executing a second manoeuvre: red points, $P_{CWC,2}$ when only the CAM for the first encounter is executed; blue points, $P_{CWC,2}$ if only the CAM for the combined primary and secondary encounter is executed; black dashed-pointed line, $P_{CWC,2}$ if only CAM for the secondary encounter is executed; dashed black line, PoC safety threshold, P_{C0} ; solid lines, evolution of $P_{CWC,2}$ as function of $\Delta\theta_{m,2}$ when executing the CAM for the secondary encounter after executing the CAM for the primary encounter (each line corresponds to a different value of $\Delta\theta_{m,1}$); shaded regions, manoeuvres violating the position constraints ($\Delta\theta_{m,2} < 4\pi$ and $\Delta\theta_{m,2} > \Delta\theta_{1,2}$).

with relative distance of 1.84 km, 5.5 revolutions after the first encounter, $\Delta\theta_{1,2} = 11\pi$ rad.

The uncertainty is modelled similarly as in the previous example. The secondary object's initial aleatory and epistemic uncertainty parameters are included in Table 3. The primary object's position is assumed to be perfectly known.

After propagating the objects' initial positions and uncertainties to the encounter times and projecting on the respective impact planes, the values included on Table 4 for uncertain variables (miss distance and covariance matrix) are obtained.

With this values, the ICS classifies both events as *Class 1*, meaning avoidance measurements are required. The same three strategies used in Example

1 are used: one manoeuvre optimising only the primary encounter, one manoeuvre optimising both encounter and one manoeuvre per encounter. The following constraints apply:

- The thruster allows to regulate the magnitude of the impulse and it is optimised so that the risk of collision drops to acceptable levels ($P_{CWC} < P_{C0} = 10^{-6}$). The maximum capacity of the thruster is $\delta v_{max} = 18\text{cm/s}$.
- No constraints on the direction are considered.
- The same restrictions on the manoeuvre execution position and restriction due to the multi-encounter as in the previous example: no ex-

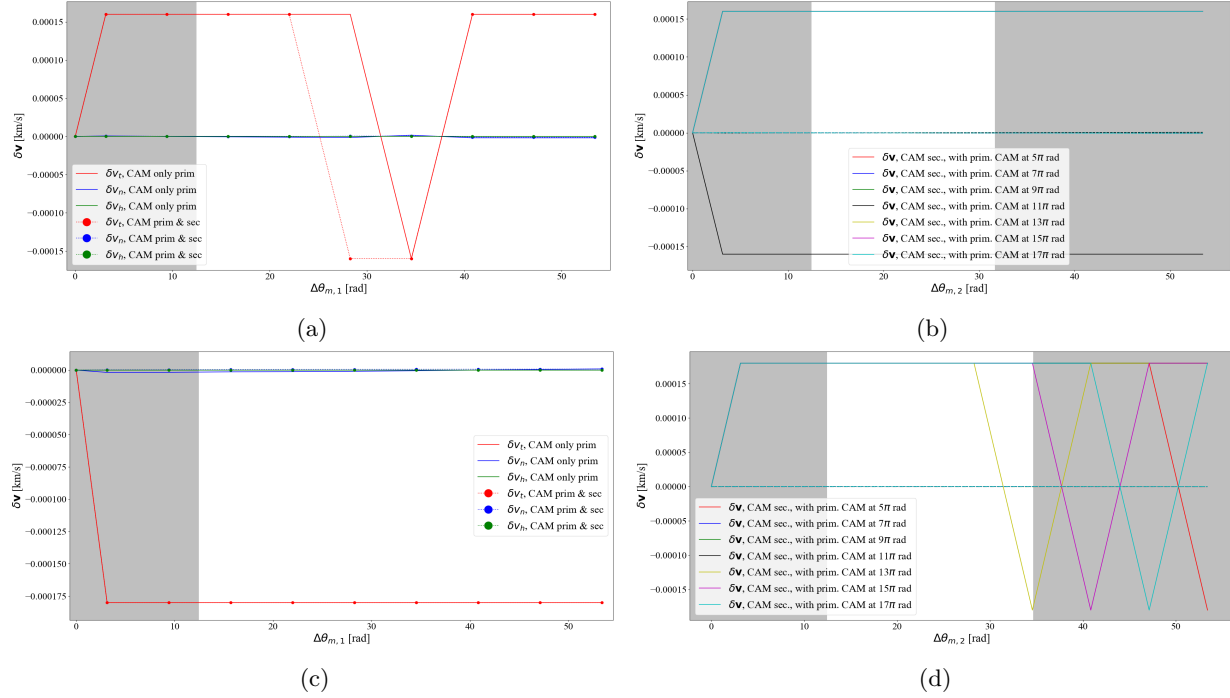


Fig. 5: Optimal impulse components, $\delta v = [\delta v_t, \delta v_n, \delta v_o]$ as a function of the execution position, $\Delta\theta_m$. (a) and (b) corresponds to the Example 1, (c) and (d) to the Example 2. (a)(c) One manoeuvre strategies: solid lines, only primary encounter; pointed lines/circles, primary and secondary encounters simultaneously; red-blue-green colours, tangential, normal and out-of-plane components, respectively; shaded region, execution manoeuvres violating the position constraints ($\Delta\theta_{m,1} < 4\pi$). (b)(d) Two manoeuvre strategies, each set of lines with same colour represent the components of the second impulse, after executing the first impulse at different values of $\Delta\theta_{m,1}$: solid lines, tangential impulses; dashed lines, normal component; dashed-pointed lines, out-of-plane component; shaded regions, execution manoeuvres violating the position constraints ($\Delta\theta_{m,2} < 4\pi$ and $\Delta\theta_{m,2} > \Delta\theta_{1,2}$). Note: all the impulses are close to a tangential impulse in the direction of the velocity (the curves overlap). Only the case when the first impulse is executed 5.5 orbits before the primary encounter (black solid line) is in the opposite direction to the orbital velocity.

ecting manoeuvres within the last 2 orbits before the encounter, and executing the second manoeuvre after the primary encounter.

A total of 42 ($N_{alt} = 42$) alternatives are obtained: 7 from the first strategy, 7 from the second strategy and 28 for the third encounter, Figs. 4 and 5 (c) and (d), numbered in the same fashion as in Example 1. The four criteria introduced in Section 4.3 are considered (in this case, the Manoeuvre Risk and the Manoeuvre Cost are not equivalent) and the collision risk criteria applies to both encounters, thus, $N_{crit} = 5$. The same two scenarios studied on the previous case are studied here. The weight distribution, including the Manoeuvre Risk criterion, is detailed in Table 5. The same liner model for normalising the matrix is employed.

Finally, the top-10 alternatives for the three scenarios ranked with the three MCDM methods detailed in Section 4.3 are included in Table 6.

5.3 Discussion of results

From this two examples, some conclusion can be derived. From the point of view of the method to obtain the robust manoeuvres to avoid a multiple encounter, it is worth noting that, at least on the proposed cases, the optimal manoeuvre is close of a tangential impulse (Fig. 5). It will be probably related with the fact that the manoeuvres are executed half an orbit before the associated encounter. In this sense, there are interesting differences between both examples when locking at the value of PoC. In Example 1, where both encounters occurs in the same orbit re-

Table 6: Top-10 alternatives for the two scenarios using the three MCDM methods considered.* *The results in Example 2 using WPM have to be treated with care since there are zeros in the normalised Decision matrix.*

Example 1						Example 2					
Scenario 1			Scenario 2			Scenario 1			Scenario 2		
WSM	WPM	TOPSIS	WSM	WPM	TOPSIS	WSM	WPM*	TOPSIS	WSM	WPM*	TOPSIS
6	6	6	8	8	8	28	28	28	8	17	8
13	13	13	1	1	1	9	33	22	1	18	1
7	7	7	9	15	9	10	17	33	2	22	2
14	14	14	2	16	2	11	22	27	9	21	9
32	32	32	3	17	15	22	18	9	3	28	3
31	31	31	17	20	16	2	27	10	10	26	17
30	30	30	15	19	17	4	38	11	4	16	18
35	35	35	16	18	3	33	26	21	11	27	16
33	33	33	10	13	10	27	32	17	17	2	15
34	34	34	6	6	11	17	31	2	18	33	10

gion, the strategies requiring one manoeuvre reduce the risk considerably for both encounters, Fig. 4a, since for both cases the manoeuvre is executed (a multiple of) half a revolution before. On the other hand, for Example 2, Fig. 4c, the first encounter risk is significantly reduced, but the risk of the second encounter is almost not affected by this single manoeuvre, even if the manoeuvre aims to optimise both encounters simultaneously.

When using the two-manoevres strategy, it can be seen that in both cases, the probability of collision of the second encounter is considerably reduced with respect to the probability of collision after the first manoeuvre, Figs. 4b and 4d, independently of the execution position of both manoeuvres. Thus, the two examples presents two very different situations from the point of view of the MCDM system: if in the first example, a manoeuvre for the first encounter is likely to be beneficial also for the second one, in the second case, the first manoeuvre may have no effect (or even a negative impact) on the second encounter and a second manoeuvre may be probably required.

Attending the results from the MCDM analysis (Table 6), before comparing both examples, some comments can be made. We have employed three different methods: WSM, WPM and TOPSIS. It can be seen from the tables that in all the scenarios but one, the three methods agree on the best solution. If attending the top-10 results, even if the order may vary from one method to another, in general, the proposed alternatives in each scenario are the same for WSM and TOPSIS. This is specially true for Exam-

ple 1. However, the WPM seems to provide slightly different alternatives, other than the best alternative. More detailed analysis is required to understand the discrepancy of this method, although one possibility may be related with the occurrence of zeros on the normalised Decision matrix.

The proximity of the rankings can be compared using the numbers of common alternatives ranked among the top-10. From Table 7 it can be seen how, in fact, WSM and TOPSIS agree better (between 8, 9 and 10 common alternatives depending on the scenario). Also, it shows that Example 1 present a better agreement among the top-10 proposed alternatives than Example 2 (up to the 10 alternatives in Scenario 1). This suggest, as expected, that Example 1 is easier to make decision on since the manoeuvre executed for the first encounter also helps the second one.

When comparing both examples, more differences can be found. When attending Scenario 1 (more weight to the PoC reduction), the top-4 alternatives in Example 1 corresponds to single-manoevres strategies, more specifically, at the earliest positions ($\Delta_{m,1} = 17\pi$ rad and $\Delta_{m,1} = 19\pi$ rad, respectively) where the PoC of both encounters drops below the threshold, Fig. 4a. Only later, alternatives with two manoeuvres appear on the list (at in any case, with an early first manoeuvre, $\Delta_{m,1} > 15\pi$, which ensures a greater reduction of $P_{C_{WC,1}}$). However, in Example 2, the situation is not so simple. The best alternative is always a two-manoevres strategy, but the top-10 alternatives are, more or less, evenly

Table 7: Number of common alternatives ranked among the top-10 between pairs of methods.

	Example 1	Example 2
Scenario 1		
WSM-WPM	10	5
WSM-TOPSIS	10	9
WPM-TOPSIS	10	5
Scenario 2		
WSM-WPM	6	3
WSM-TOPSIS	9	8
WPM-TOPSIS	5	4

distributed between single or multiple manoeuvre strategies (excluding WPM ranking). This is related with: first, the fact that none of the proposed alternatives achieved $P_{C_{WC,2}} < P_{C_0}$ and, second, that a single manoeuvre does not reduce significantly the risk of the second encounter, see Fig. 4d.

When prioritising the cost of the manoeuvre (Scenario 2), both examples behave similarly. In fact, the 4 or 5 best alternatives in both scenarios with WSM and TOPSIS are the same: a single manoeuvre executed close to the event ($\Delta_{m,1} = 5\pi$ rad and $\Delta_{m,1} = 7\pi$ rad, respectively). This makes sense: a single manoeuvre has a lower Manoeuvre Risk associated, and late manoeuvres have a smaller impact on the Operational Cost. It is worth noting how the best alternatives differ with respect to Scenario 1 and, in fact, do not accomplish $P_{C_{WC,1}} < P_{C_0}$ and $P_{C_{WC,2}} < P_{C_0}$. This highlights the challenging environment operators face when selecting the best strategy to deal with a multi-encounter event when conflict criteria are considered.

Finally, it would be interesting to analyse the similarity between the top ranked alternatives. For instance, in the Scenario 2, in both examples, the top ranked solutions are: 8, 1, 9, 2. However, solutions 8 and 1 are single-manoevr approaches executing 2.5 revolutions before the encounter. The only difference is that Alternative 1 is computed optimising only the first encounter and Alternative 8 optimising both encounter simultaneously (and similar for alternative 2 and 9, but executing the manoeuvre 3.5 revolution before the encounter): both alternatives propose a similar CAM, almost a tangential impulse in the same direction (Fig. 5), and the reduction of the probability of collision is also the same (Fig. 4). A similar conclusion can be reached with the top alternatives in Scenario 1 of Example 1. Thus, it would be inter-

esting to include a final step on the decision-making system that filters the ranked alternatives according to the similarity to the solutions listed immediately above attending to their proximity as proposed in Ramirez-Atencia et al.¹⁸

6. CONCLUSIONS

This paper introduces a decision-making system to support operators with CAM allocation tasks in the event of a multiple encounter scenario.

We have extended a robust CAM optimisation method, which accounts for aleatory and epistemic uncertainty on the objects' position, to the multi-encounter case. We have also shown that the model can respond to different strategies depending on the number of manoeuvres to implement, providing optimal solutions in all of them. We have also included operational constraints on the optimisation. We have illustrated the robustness of the solution with any of the strategies with two numerical examples.

We have also presented an improvement on an intelligent decision support system to help on the allocation of avoidance manoeuvres. More specifically, we have applied the system to the multiple-encounter scenario. In this work we have added a new layer of decision-making based on MCDM that allows to rank the best alternatives computed with the robust CAM optimisation method. We have tested the system on two different scenarios: an easier one where both encounters occur in the same region of the orbits, and a second more challenging one where the encounters happen at opposite sides of the orbits. We have demonstrated the importance of the multiple-encounter geometry on the CAM allocation decision. The system has been proved to provide the expected results under different scenarios proposed: prioritising the collision risk reduction or giving more importance to the associated cost of the strategy. Different MCDM methods have been employed given coherent results among them.

Nevertheless, a deeper analysis of the MCDM capacities has to be performed in order to understand the behaviour of the decision-making system under different circumstances (criteria, normalisation models, methods...). Also, a further layer on the decision-making process would be beneficial to filter those ranked solutions that are too similar in order to provide the operators with a truly wider range of alternatives. After this, the next step would be to extend the model to the LT scenario.

ACKNOWLEDGMENT

This work was funded by the Open Space Innovation Platform (OSIP) of the European Space Agency (ESA), Idea I-2019-01650: “Artificial Intelligence for Space Traffic Management”

REFERENCES

- [1] ESA Space Debris Office ESA/ESOC. ESA’s Annual Space Environment Report. May 2021.
- [2] M. Balch, R. Martin, and S. Ferson. Satellite Conjunction Analysis and the False Confidence Theorem. *Proceedings of the Royal Society A: Mathematical, Physical and Engineering Sciences*, 475, July 2019.
- [3] L. Sánchez and M. Vasile. On the Use of Machine Learning and Evidence Theory to Improve Collision Risk Management. *Acta Astronautica*, 181:694–706, 2020.
- [4] G. Shafer. *A Mathematical Theory of Evidence*. Princeton University Press, 1976, Princeton, NJ, 1 edition, April 1976.
- [5] L. Sánchez and M. Vasile. Intelligent Agent for Decision-making Support and Collision Avoidance Manoeuvre Design. *Acta Astronautica*, Under review, 2021.
- [6] L. Sánchez and M. Vasile. AI for Autonomous CAM Execution. *71st International Astronautical Congress. The CyberSpace Edition*, 2020.
- [7] E. Triantaphyllou. *Multi-Criteria Decision Making Methods*, pages 5–21. Springer US, Boston, MA, 2000.
- [8] M. Vasile and C. Colombo. Optimal Impact Strategies for Asteroid Deflection. *Journal of Guidance, Control and Dynamics*, 31(4):858–872, 2008.
- [9] R. Serra, D. Arzelier, M. Joldes, J.B. Lasserre, A. Rondepierre, and B. Salvy. Fast and Accurate Computation of Orbital Collision Probability for Short-Term Encounters. *Journal of Guidance, Control, and Dynamics*, 39:1–13, January 2016.
- [10] K. Merz, V. Braun, V. Benjamin Bastida, T. Flohrer, Q. Funke, H. Krag, and S. Lemmens. Current Collision Avoidance service by ESA’s Space Debris Office. *7th European Conference on Space Debris, Darmstadt, Germany*, 2017.
- [11] E. Triantaphyllou, B. Shu, S. Nieto Sánchez, and T. G. Ray. *Multi-criteria Decision Making: An Operations Research Approach*, pages 175–186. John Wiley & Sons, New York, NY, 1998.
- [12] T.M. Lakshmi, Vetrivel K., A. Joshuva Anand, and V. Prasanna Venkatesan. A Study on Different Types of Normalization Methods in Adaptive Technique for Order Preference by Similarity to Ideal Solution (TOPSIS). *International Journal of Engineering Research & Technology (IJERT) NCETCS*, 4, 2016.
- [13] A. Kolios, V. Mytilinou, E. Lozano-Minguez, and K. Salonitis. A Comparative Study of Multiple-Criteria Decision-Making Methods under Stochastic Inputs. *Energies*, 9:566, 2016.
- [14] J.R.S.C. Mateo. Weighted Sum Method and Weighted Product Method. *Multi Criteria Analysis in the Renewable Energy Industry. Green Energy and Technology*, 160, 2012.
- [15] C. Tofallis. Add or Multiply? A Tutorial on Ranking and Choosing with Multiple Criteria. *INFORMS Transactions on Education*, 14(3):109–119, 2014.
- [16] S. García-Cascales and T. Lamata. On Rank Reversal and TOPSIS Method. *Mathematical and Computer Modelling*, 56(5):123–132, 2012.
- [17] K. Sentz and S. Ferson. *Combination of Evidence in Dempster-Shafer Theory*. January 2002.
- [18] C. Ramirez-Atencia, V. Rodriguez-Fernandez, and D. Camacho. A revision on Multi-Criteria Decision Making methods for Multi-UAV Mission Planning Support. *Expert Systems with Applications*, 160, July 2020.